The Meteoritical Society

Meteoritics & Planetary Science 42, Nr 11, 1915–1927 (2007)
Abstract available online at http://meteoritics.org

The effect of the oceans on the terrestrial crater size-frequency distribution: Insight from numerical modeling

Thomas DAVISON and Gareth S. COLLINS*

Impacts and Astromaterials Research Centre, Department of Earth Science and Engineering, Imperial College London, South Kensington Campus, London, SW7 2AZ, UK
*Corresponding author. E-mail: g.collins@imperial.ac.uk

(Received 16 October 2006; revision accepted 08 May 2007)

Abstract–On Earth, oceanic impacts are twice as likely to occur as continental impacts, yet the effect of the oceans has not been previously considered when estimating the terrestrial crater size-frequency distribution. Despite recent progress in understanding the qualitative and quantitative effect of a water layer on the impact process through novel laboratory experiments, detailed numerical modeling, and interpretation of geological and geophysical data, no definitive relationship between impactor properties, water depth, and final crater diameter exists. In this paper, we determine the relationship between final (and transient) crater diameter and the ratio of water depth to impactor diameter using the results of numerical impact models. This relationship applies for normal incidence impacts of stoney asteroids into water-covered, crystalline oceanic crust at a velocity of 15 km s^{-1}. We use these relationships to construct the first estimates of terrestrial crater size-frequency distributions (over the last 100 million years) that take into account the depth-area distribution of oceans on Earth. We find that the oceans reduce the number of craters smaller than 1 km in diameter by about two-thirds, the number of craters ~30 km in diameter by about one-third, and that for craters larger than ~100 km in diameter, the oceans have little effect. Above a diameter of ~12 km, more craters occur on the ocean floor than on land; below this diameter more craters form on land than in the oceans. We also estimate that there have been in the region of 150 impact events in the last 100 million years that formed an impact-related resurge feature, or disturbance on the seafloor, instead of a crater.

INTRODUCTION

Oceans cover 70% of the Earth, implying that most meteoroid impacts occur in water-covered targets. However, of the ~170 known or suspected impact structures on Earth, only 15–20 are thought to have formed in a marine environment (Ormö and Lindstrom 2000), and the majority of these are now on land. The paucity of marine craters is in part due to of the water layer inhibiting or altering the cratering process and also in part due to the young age of the oceanic crust (the oldest seafloor is only approximately 180 million years old due to the continuous recycling of oceanic crust through seafloor spreading and subduction). Of the known marine-impact structures, all but one formed a detectable crater in the seafloor, the exception being the Eltanin structure in the Bellingshausen Sea, Antarctica (Kyte et al. 1981). This is the only deep-sea impact event known, despite the fact that deep ocean basins cover approximately 60% of the Earth's surface. Another reason for the small number of known marine impact structures, therefore, is simply that they have not been discovered because of insufficient geophysical or bathymetric mapping of the sea floor. This observation naturally raises the question of how many impact craters we should expect to find on the seafloor today. The answer has important implications for interpreting the terrestrial cratering record and correlating the crater size-frequency distribution with impactor flux.

Since very few marine-environment craters are known, they are not very well understood, but are perhaps more important than the quantity of work suggests. They are, after all, the most likely type of impact to occur in the future, and there are obvious geohazards associated with them—for instance, the formation of large-scale tsunami (Nemtchinov et al. 1996). In recent years, much progress has been made in the qualitative understanding of how a water layer affects the impact process. The interpretation of geological and geophysical data at known marine-target craters provides enlightening comparison with what is known about sub-aerial craters. For example, Ormö and Lindstrom (2000) suggested that terrestrial craters formed in deep marine environments

Table 1. Model parameters used in this work.

Parameter	Value
Poisson's ratio (water)[a]	0.5
Poisson's ratio (granite)[a]	0.25
Coefficient of friction (intact granite)[a]	1.5
Coefficient of friction (damaged granite)[a]	0.6
Cohesion (intact granite)[a]	5×10^7 Pa
High-pressure strength limit (granite)[a]	2.5×10^9 Pa
Melt temperature (granite)[a]	1500 K
Melt temperature (water)[a]	273 K
AF-model viscosity parameter[b]	0.05
AF-model decay time parameter[b]	200
Impactor velocity	15 km s^{-1}
Impactor density	2680 kg m^{-3}
Resolution	15 cppr

[a]See Collins et al. (2004) for a description of the strength-model parameters.
[b]See Wunnemann and Ivanov (2003) for details of the acoustic fluidization scaling.

frequently lack melt sheets and a topographic crater rim, but have internal deposits and radial gullies formed by resurge of the sea. Based on the interpretation of seismic data and drill cores at the Mjølnir (Tsikalas 1996) and Chesapeake Bay (Poag 1996) craters, marine-target craters appear to be broader than their subaerial counterparts, which is believed to be a consequence of the resurging water action and/or the low strength of near-surface submarine sediments (Shuvalov et al. 2002; Poag et al. 2004; Collins and Wünnemann 2005).

Previous experimental and numerical modeling work has shown that the effect of a water layer on crater formation is most sensitively controlled by the ratio between the water depth and the impactor diameter—referred to hereafter as R (for example, Gault and Sonnett 1982; Shuvalov 2002; Shuvalov et al. 2002; Shuvalov and Trubestkaya 2002; Ormö et al. 2002; Ormö and Miyamoto 2002; Wünnemann and Lange 2002). However, a definitive relationship between final crater diameter and R has not yet been established. By simulating the impact of an impactor 200 m in diameter at 15 km s^{-1} into water-covered targets, Shuvalov (2002) showed that a shallow water layer ($R < 0.5$–1) has little effect on the cavity forming in the basement; that for $R > 2$, cavity size is reduced as the impactor is completely decelerated, deformed, and disrupted during penetration of the water layer; and that for $R > 4$, no crater occurs on the seafloor. Artemieva and Shuvalov (2002) also found from their numerical models that for $R > 4$, a submarine crater is almost nonexistent (for an impactor 1 km in diameter with an impact velocity of 20 km s^{-1}); however, the marine-impact models of Wünnemann and Lange (2002) did show significant disturbance of the seafloor for $R = 5$ (using the same impactor size and velocity). Laboratory-scale impact experiments (Gault and Sonnett 1982; Baldwin et al. 2007) provide further quantitative analysis of the effect of water layer thickness on crater size, albeit at a much smaller scale and lower velocity than typical marine craters. Results from these experiments suggest that craters may form in the target beneath water of depths up to 10–20 times the diameter of the impactor (R = 10–20).

The purpose of this paper is to quantify the relationship between crater diameter and the ratio between water depth and impactor diameter by numerically simulating oceanic impact events. We then use this relationship to examine the effect of the Earth's oceans on the global crater size-frequency distribution and estimate how many craters we should expect to find on the ocean floor today.

METHOD

To determine a quantitative relationship between crater diameter and the ratio of ocean water depth to impactor diameter, we simulated over 60 marine-target impact events using the iSALE hydrocode (Wünnemann et al. 2006), a multi-material, multi-rheology impact model based on the SALE hydrocode (Amsden et al. 1980). iSALE is a well-established code that has been used to simulate several terrestrial impact events (Artemieva et al. 2004; Collins et al. 2002; Collins and Wünnemann 2005; Ivanov 2005; Ivanov and Artemieva 2002; Ivanov and Deutsch 1999; Wünnemann et al. 2005), including targets with a water layer (Wünnemann and Lange 2002; Collins and Wünnemann 2005), and develop a generic, quantitative model for the formation of impact craters in crystalline targets (Wünnemann and Ivanov 2003). iSALE is similar in many regards to the SOVA hydrocode used to simulate marine-target impacts in many previous modeling studies (Shuvalov 1999, 2002; Artemieva and Shuvalov 2002; Shuvalov et al. 2002; Shuvalov and Trubestkaya 2002). The two models differ in the details of their solution algorithms (SOVA uses a wider finite-difference stencil and more accurate advection scheme) and in the way in which they model target strength (iSALE includes a somewhat more realistic elastic-plastic rock strength model—see below).

For all simulations described here, the ANEOS equations of state for granite and water were used to represent the seafloor and ocean. Granite was chosen because, unlike basalt, it has a well-defined Equation of State (EoS) and constitutive model, and because the constitutive model parameters for basalt and granite are similar. The constitutive model used is described in Collins et al. (2004) and Ivanov et al. (1997); it defines the rock strength to be a function of pressure, temperature, and plastic strain, based on laboratory-derived strength measurements. The water is modeled as an inviscid fluid. As in previous work, a transient weakening mechanism was necessary to facilitate late-stage collapse of the crater and produce the required final complex crater form. In our work, this was achieved using the acoustic fluidization model (Melosh and Ivanov 1999; Ivanov and Artemieva 2002). The scaling of the model parameters used to correctly simulate the size morphology progression of terrestrial craters is described by Wünnemann and Ivanov (2003). The

important model parameters used in this work are listed in Table 1.

In dry impacts (those without a water layer) under constant gravity, the final crater diameter in a common target material depends only on the impactor properties (size, density, and velocity of the impactor and the angle that its trajectory makes with the target surface). In oceanic impacts, an additional controlling factor is the depth of the water layer. In our investigation, we chose to keep the density and velocity of the impactor fixed and vary only the impactor diameter and the depth of the water layer. We used an impact velocity of 15 km s^{-1}, which is within the range of typical velocities for impacts on Earth (12–20 km s^{-1}; Bottke et al. 1995). Fireballs with asteroidal sources (and therefore larger asteroids as well) have a median (and mean) velocity at the top of the Earth's atmosphere of ~18 km s^{-1} (Halliday et al. 1996). We used a slightly lower impact velocity, and consequently a slightly larger projectile size, as a compromise to maximize the mesh resolution over the projectile. For convenience, the impactor density used was 2680 kg m^{-3}, which is equivalent to that of a porous stony asteroid, to allow the same material (granite) to be used for the impactor and seafloor. The angle of impact in all simulations was perpendicular to the target surface, enforced by the axisymmetric nature of the model. The assumption of vertical impact is unrealistic; moderately oblique impacts (40–50°) are six times more common than near-normal incidence impacts (80–90°). However, the fact that, for impact angles greater than ~10° to the horizontal all impact craters are circular in plan, and that no observable structural crater feature has yet been unequivocally linked to impact direction or angle, suggests that the approximation of impact cratering as an axisymmetric process is a good one.

Three sets of simulations were performed, each with a fixed impactor diameter (L = 100 m, L = 500 m, and L = 1 km), to investigate the effect of water layer thickness on crater formation over a range in impactor sizes. The three impactor diameters were chosen to span the range of terrestrial impact events where the effect of a water layer is important, and to keep the maximum water depth investigated within reason. At the lower end, stony impactors much smaller than 100 m in diameter are significantly affected by atmospheric entry (broken up and/or decelerated) and will probably not form a single large impact crater. At the upper end, the maximum depth of the terrestrial oceans (~7 km) implies that a large range in R cannot be achieved for impactors much greater than 1 km in diameter. The range of impactor sizes investigated also included impacts that form both simple and complex craters. Simple craters are bowl-shaped depressions, with a raised rim and a depth-to-diameter ratio of about 0.2, that form on Earth with diameters smaller than ~2–4 km (Dence 1965). Complex craters are larger. In this case, the deep cavity formed during impact appears to be unstable: the rim of the crater collapses inward and the floor of the crater uplifts to form a central peak or ring of peaks. The depth-to-diameter ratio of complex craters is substantially smaller than for simple craters (Dence 1965). In each set of simulations, we kept the resolution (number of cells per projectile radius) constant and varied the water thickness from 0–8 times the impactor diameter (at water thicknesses in excess of ~8 L, no crater forms on the seafloor). The results from each numerical simulation were processed to extract the morphology and dimensions of the crater in the seafloor at regular intervals during the formation of the crater.

RESULTS

Figures 1 and 2 illustrate the qualitative effect of increasing water depth on crater formation for an impactor 100 m and 1 km in diameter. The simulations with L = 500 m produced similar results to those with L = 1 km and for brevity are not shown. The top row in each figure shows the initial conditions, the second row shows an intermediate stage of the growth of the crater when it has reached its maximum depth in the seafloor, and the bottom row shows the final, collapsed crater morphology. In agreement with previous modeling studies, our results suggest that the presence of a water layer affects an impact event in two important ways. First and foremost, the water layer changes the coupling of the impactor's kinetic energy to the seafloor. In other words, the thicker the water layer, the smaller the fraction of the impactor's kinetic energy that is transferred to the seafloor. The second effect of a water layer on the impact process is to influence the collapse of the crater in the seafloor. The importance of this effect ranges from minor rim modification to extreme modification of the seafloor and enhancement of gravitationally driven collapse of the crater in the seafloor.

The first column of each figure shows the intermediate and final morphology of the crater formed when no water layer is present. In each case, the intermediate form, often termed the transient cavity, is qualitatively the same: a deep, bowl-shaped depression with a constant depth-to-diameter ratio. However, the final crater form in each case is qualitatively different, in accordance with terrestrial and extraterrestrial observation. In Fig. 1, the final crater, which is 1.55 km in diameter (measured at the pre-impact surface), is a simple, bowl-shaped crater with a floor-covering of debris that has slumped down from the crater rim; in Fig. 2, more dramatic collapse of the transient crater has occurred, resulting in a broader final crater and uplift of the crater floor, forming a central peak.

The Effect of the Water Layer on Crater Growth and Transient Crater Size

The most important effect of the water layer on the impact process is the dissipation of the impactor's kinetic energy. As the water layer thickness increases, the dimensions of the crater formed on the seafloor at the time

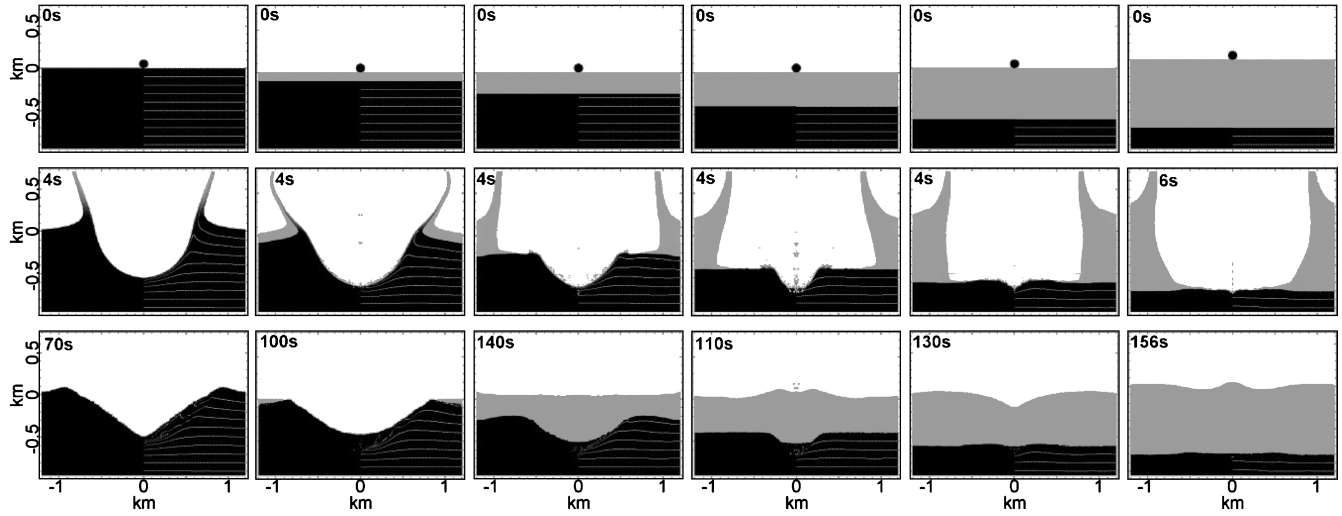

Fig. 1. Model results for simulations of impactors 100 m in diameter. The top row shows the initial case for each simulation the instant before the collision between the impactor and the target. The second row displays the point in the simulation at which the maximum depth of the cavity in the basement rock is reached. The bottom row shows the final state of the simulation after the collapse stage of the cratering process. Water depth increases from left to right; the *R* values for each column are 0, 1, 2.5, 4, 6, and 8. The shade of gray is indicative of the density of the material (darker gray is denser material). The dashed pale gray lines represent the positions of massless tracers that follow the particle paths of target material through time.

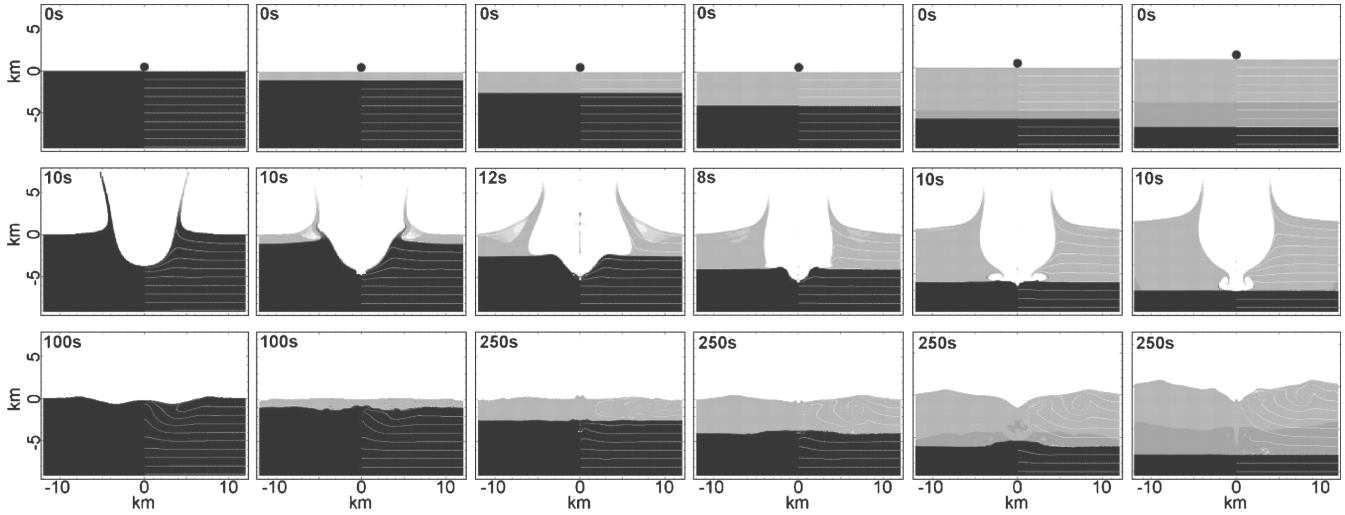

Fig. 2. As in Fig. 1, but for impactors 1 km in diameter.

of maximum crater depth decrease despite little change in the diameter of the cavity formed in the water layer at similar instances in time. This is illustrated qualitatively by the reduction in size of the crater in the seafloor looking from left to right along the middle row of Figs. 1 and 2. The quantitative relationship between transient crater depth and the ratio of water depth to impactor diameter is shown in Fig. 3; it is remarkably similar for each impactor size. Despite the obvious monotonic reduction in transient crater size with increasing water depth, the physical explanation for this relationship is not straightforward. It is overly simplistic to consider the effect of the water layer as merely decelerating the impactor by drag forces during its passage from the sea surface to the seafloor. The impactor and water near the point of contact are actually rapidly compressed and decompressed, forming a shock wave that traverses the water layer and passes into the seafloor ahead of the impactor. In addition, as the impactor penetrates the water layer, it is flattened and breaks up, which further decelerates it. As a result, impact-induced movement of the seafloor can begin well before the impactor reaches the seafloor.

However, by assuming that the only effect of the water layer is to reduce the kinetic energy deposited on the seafloor, it is possible to derive a theoretical approximation of the relationship between *R* and the ratio of the size of the transient crater formed in the seafloor to the size of the transient crater

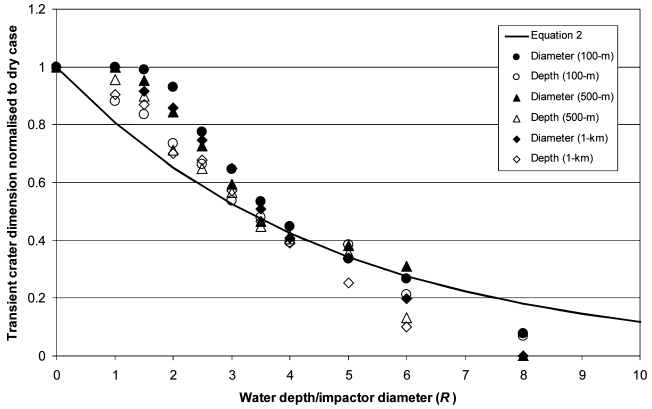

Fig. 3. Plot of cavity dimensions (at the time of maximum crater depth) normalized to the dimension of the cavity with no water layer as a function of relative water depth R. Included are depth and diameter measurements for all three sets of simulations (for impactor diameters 100 m, 500 m, and 1 km). Also plotted for comparison is a theoretical scaling law (Equation 2) derived assuming that cavity size is affected only by kinetic energy loss of the impactor during penetration of the water column. See text for further discussion.

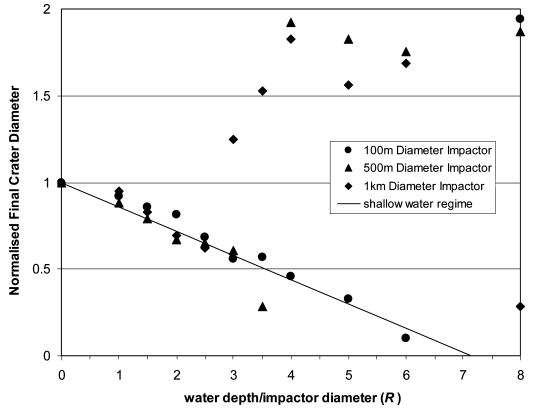

Fig. 4. Plot of final crater diameter, normalized by the diameter of the crater formed when no water layer is present, as a function of relative water depth R (for impactor diameters of 100 m, 500 m, and 1 km). The craters formed within the shallow water regime (see text for further discussion) are well fit by the straight line plotted (Equation 3).

formed in an identical target with no water layer. If the only difference between two impacts is the impactor velocity, the pi-group scaling laws of Schmidt and Housen (1987) can be rearranged to show that the ratio of the transient crater diameters (or depths) in each impact is equal to the ratio of the impact velocities raised to the power of 2β, and by inference, the ratio of the impactor kinetic energies to the power of β, where β is a material-specific scaling exponent (Schmidt and Housen 1987; Melosh 1989, p. 119, Table 7.1). Thus, by assuming that traversing the water layer simply reduces the velocity of the impactor, from v_0 at the surface to v on the seafloor, the relative reduction in transient crater size is given by the kinetic energy loss during penetration of the water layer (E/E_0), to the power of β.

$$\frac{D_{tc}^{wet}}{D_{tc}^{dry}} = \left(\frac{v}{v_0}\right)^{2\beta} = \left(\frac{E}{E_0}\right)^{\beta} \quad (1)$$

Kinetic energy loss of an impactor as a function of penetration depth can be derived from equations describing the drag on a rigid sphere moving at supersonic speeds through a fluid (O'Keefe and Ahrens 1982; Wünnemann and Lange 2002; their Equation 8). Substituting this equation into Equation 1, gives:

$$\frac{D_{tc}^{wet}}{D_{tc}^{dry}} = \exp\left(-\beta\frac{3c_d\rho_w}{\rho_i}R\right) \quad (2)$$

where c_d is the drag coefficient (0.877 for a rigid sphere), ρ_w is the water density, and ρ_i is the impactor density.

Equation 2 (for β = 0.22; suitable for solid rock in the gravity regime) is also plotted on Fig. 3; it is a reasonable fit to the data over an intermediate range of water depths ($3 < R < 6$). In deeper water, the modeled transient crater dimensions are smaller than predicted by Equation 2, probably because the simple scaling law does not take into account the increased deceleration of the impactor as it spreads and breaks up during penetration of the water layer. In shallow water, the modeled transient crater dimensions are slightly greater than predicted by Equation 2. This is most likely because our simple approximation inadequately accounts for the complex initial coupling of the impactor and water layer in which the projectile is still moving at hypersonic, not supersonic velocity. Indeed, we find that the maximum kinetic energy of the water layer is not achieved until the impactor has penetrated to about twice its diameter and lost about 80% of its initial kinetic energy. Although it is not shown in Fig. 3, the experimental data for crater size versus R described in Baldwin et al. (2007) lie well above our modeling results. The main reason for this is probably the greater difference in density between the impactor and water in their experiments (they used stainless steel impactors), although the experiments also differ considerably from our model simulations in terms of projectile size, projectile velocity, and the target property controlling crater growth in the rock (strength in the case of the experiments; gravity in the case of the models). We find that Equation 2 fits the data of Baldwin et al. (2007) reasonably well (for $R < 6$) using = 0.28, suitable for solid rock in the strength regime (see Melosh 1989, p. 119, Eq. 7.7.13 [note that this equation is wrong by a factor of −1]), and ρ_i = 7800 kg m^{-3}. Comparison between our transient crater measurements and their final crater measurements (taking into account the different cratering regimes) is appropriate given the absence of crater collapse at the laboratory scale.

The Effect of the Water Layer on Crater Collapse and Final Crater Size

Figure 4 shows our model results of the final crater diameter, normalized to the final crater diameter of the dry case ($R = 0$) as a function of R. Final crater diameters and the normalized values are also listed in Table 2. For the simple crater case (impactor 100 m in diameter; Fig. 1), the final crater diameter decreases linearly with increasing R until no crater is formed in the seafloor (last column of Fig. 1). In the two larger-impactor cases, which form complex final craters (e.g., Fig. 2), a very similar relationship between final crater diameter and R exists for shallow water depths ($R < 3$ for impactors 1 km in diameter and R < 4 for impactors 500 m in diameter). Using just these data points, and performing a linear regression, we find that the ratio of final crater diameters between the water layer and the no water layer is given by the equation:

$$\frac{D_f^{wet}}{D_f^{dry}} \approx 1 - 0.14R \quad (3)$$

This is shown as the solid line in Fig. 4. The goodness of fit is quantified by the coefficient of determination (R^2), which has a value of 0.92.

For the simple crater simulations and the complex crater simulations for $R < 3$, the presence of the water layer does not substantially alter the gross characteristics of the final crater morphology, although there are important fine-scale but geologically observable differences apparent. In other words, the resurging water makes only a minor modification to the rim as it flows back into the cavity; the effect on the late-stage collapse of the crater is small. However, for the complex crater simulations (impactors 500 m and 1 km in diameter), there is a qualitative change in the crater-formation process when the water depth exceeds ~3 times the impactor diameter. At these depths, the resurging water starts to substantially affect the late-stage modification of the crater and produces final crater morphologies unlike conventional terrestrial and extraterrestrial craters. As the resurge flow moves back toward the center of the crater, seafloor material outside the transient crater rim is moved (scoured) by the high-velocity water flow, forming a very shallow depression in the sea floor outside the transient crater. In addition, the crater rim is eroded and the uplift of the central mound inside the crater is enhanced, such that the central region of the crater is often above the pre-impact seafloor level. Figure 5 illustrates the final crater morphology from three simulations of impactors 1 km in diameter with water depths of 0, 1, and 3 km. In cases where the final "crater" morphology has a central topographic high and an external topographic low, the diameter of the outer limit of this external depression is plotted as the final crater diameter in Fig. 4.

Although thought-provoking, we do not consider the apparent scouring of the seafloor during these large, deep-water impact models to be a robust result. The depth of the depression in the seafloor is close to the limit of resolution (the minimum cell size in the mesh), and the extremely complex interaction at the interface between the water and the seafloor is oversimplified in our model. Furthermore, as our 2-D numerical model confines the motion of the water to be radial and axisymmetric, it is unclear how the resurge flow would manifest itself in three dimensions. As the transient crater in the water column collapses and the water begins to flow back into the center of the crater, the water may not flow back in through all degrees of the circle equally. Along certain azimuths, perhaps defined by weaknesses in the underlying seafloor material, the water may carve resurge gullies through the crater rim, as proposed at the Lockne crater in Sweden (von Dalwigk and Ormö 2001; Ormö and Miyamoto 2002). Once formed, the water would primarily flow back into the crater through these gullies, with the rim and surrounding seafloor experiencing less erosion in other places.

The complex crater simulations show a further interesting change in behavior for water depths between $R = 6$ and $R = 8$ (above $R = 8$, the effects of the impact on the seafloor are no longer discernable). At this range of relative water depths, insufficient energy from the impact reaches the ocean floor to form a crater; however, the shockwave generated by the collision between the impactor and the water still reaches the seafloor with sufficient strength to have an observable effect on the ocean floor. The calculated plastic strain in the seafloor shows that the energy reaching it is enough to fracture the rock and hence weaken it relative to its pre-impact state. As the water cavity forms above the fractured seafloor, the substantial weight of the water column is temporarily removed, allowing the most intensely fractured and weakened rock in the center of the impact site to isostatically adjust, forming an uplift on the ocean floor. In the simulation of an impactor 1 km in diameter into an ocean 6 km deep, the uplift was approximately 600 m high and remained as positive relief for the duration of the simulation (250 s).

To summarize the qualitative effect of the water layer on final crater morphology observed in our model results, three regimes of behavior can be identified and are summarized in Fig. 6. As R increases from zero, the size of the crater (particularly the diameter) decreases. This regime (defined here as the shallow water regime) appears to extend to higher R values for smaller impacts (those forming simple craters) than larger ones. This is consistent with previous modeling results (Shuvalov 2002), which showed that a shallow water layer ($R < 1$) has little effect on the cavity forming in the basement, and that for $R > 2$, cavity size is reduced as the impactor is completely decelerated, deformed, and disrupted during penetration of the water layer. An intermediate water depth regime exists in the range $3–4 < R < 6–8$ for impactors that

Table 2. Final crater diameters derived from simulation results (measured at the level of the pre-impact seafloor). Also shown is the normalized crater diameter (i.e., the final crater diameter divided by the corresponding crater formed when no water is present).

	100 m		500 m		1 km	
R	Crater diameter (km)	Final diameter/ dry diameter	Crater diameter (km)	Final diameter/ dry diameter	Crater diameter (km)	Final diameter/ dry diameter
0	**1.55**	1.000	**7.55**	1.000	**13.40**	1.000
1	**1.43**	0.923	**6.65**	0.881	**12.70**	0.948
1.5	**1.33**	0.858	**5.95**	0.788	**11.10**	0.828
2	**1.26**	0.813	**5.05**	0.669	**9.30**	0.694
2.5	**1.06**	0.684	**4.90**	0.649	**8.30**	0.619
3	**0.87**	0.561	**4.60**	0.609	16.70	1.246
3.5	**0.88**	0.568	**2.15**	0.285	20.50	1.530
4	**0.71**	0.458	14.50	1.921	24.50	1.828
5	**0.51**	0.329	13.80	1.828	20.90	1.560
6	**0.16**	0.103	13.25	1.755	22.60	1.687
8	3.01	1.942	14.10	1.868	3.80	0.284

Diameter values in bold are those used in the linear regression defining Equation 3. Diameter values not in bold represent the diameter of the impact-related resurge feature where no conventional crater exists (see text for further explanation).

form complex craters. In this regime, gravitational collapse and isostatic rebound of the crater floor removes the topographic low in the center of the crater, leaving a central uplifted region. Resurge of the water column back into the crater is also significant, probably leaving a broad high-energy water flow feature on the ocean floor (the nature of which cannot be determined by axisymmetric modeling). Shuvalov (2002), using an impactor 200 m in diameter, suggested that no crater would form in this regime. Artemieva and Shuvalov (2002) found from their numerical models that for an impactor 1 km in diameter and $R > 4$, a submarine crater is almost nonexistent, but they did not note any such scour crater or large central uplift. However, the marine impact models of Wünnemann and Lange (2002) showed "significant particle movement within a distance of 15 km from the impact centre" for an impactor 1 km in diameter and $R = 5$, despite no permanent crater forming in the seafloor. A final regime—the deep water regime—is observed in our models for $R > 8$; in this case, the water layer completely dissipates the energy of the impactor, and no trace of the impact is observable on the seafloor. Laboratory-scale impact experiments (Gault and Sonnett 1982; Baldwin et al. 2007) suggest that the deep-water regime may not begin until $R \sim 10$.

The Effect of the Oceans on the Terrestrial Crater Size-Frequency Distribution

Using the quantitative relationship established by our numerical modeling, which relates final crater diameter to the ratio of water depth and impactor diameter (Equation 3), it is possible to examine the effect of the Earth's oceans on the predicted terrestrial crater size-frequency distribution. To achieve this, we constructed a simple statistical model of impacts on Earth. The model requires a size-frequency distribution of terrestrial impactors, a depth-area distribution of oceans and seas over the globe, and equations to determine the final crater diameter from the impactor diameter and water depth. The model works by repeatedly selecting a random impactor diameter and random ocean depth, and computing the appropriate final crater diameter for a dry or water-covered target to build up a cumulative picture of the effect of the oceans on the crater size-frequency distribution. Because of the young age of the seafloor in comparison to that of the continents, we restricted our application of the model to a time period of 100 million years, the approximate average age of the seafloor.

We considered two size-frequency distributions of impactors reaching the Earth's surface over the last 100 Ma as inputs into our model. One was a simple power-law fit to observational data compiled by the Near-Earth Object Science Definition Team (2003); in this case, the number of impactors N (>L) with diameters larger than L (in m) is given by:

$$N\,(>L) = 2 \times 10^{9} L^{-2.34} \tag{4}$$

The other was derived from a predicted crater size-frequency distribution based on a range of data from fireball observations and models of atmospheric entry of meteorites to terrestrial crater counts, and using a fit consistent with the lunar production function (Bland 2005; Bland and Artemieva 2003, 2006). In this case, for impactors larger than 50 m in diameter, N (>L) is well approximated by:

$$N\,(>L) = \frac{3 \times 10^{9} L^{-2.94}}{5.7 \times 10^{4} L^{-2.23} + L^{-0.71}} \tag{5}$$

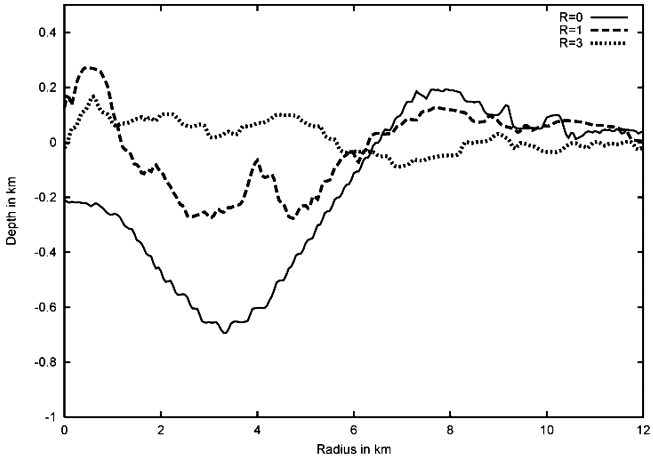

Fig. 5. Vertically exaggerated final crater profiles for craters formed by an impactor 1 km in diameter in targets with a water depth of 0, 1, and 3 km (R = 0, 1, and 3). The center of the crater is on the left side of the plot. The R = 0 profile displays a typical complex crater profile, with a central peak and a raised rim. The R = 1 profile is qualitatively similar, but with a smaller crater diameter (as measured at the pre-impact seafloor) and an enhanced central uplift. The R = 3 profile is qualitatively very different; the crater is replaced by a central mound and surrounded by a shallow depression (between approximately 6 and 8 km in radius) formed by the resurging water column. See text for further discussion.

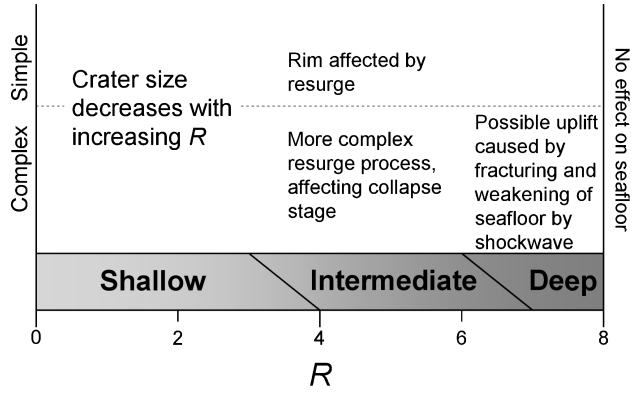

Fig. 6. Diagram summarizing the influence of the water column on the marine-cratering process as a function of crater size and R (the ratio of water depth to impactor diameter). Three regimes of qualitative behavior are observed.

Two impactor populations (with the smallest impactor diameters at 50 m) were defined based on these size-frequency distributions; the power-law population contained nearly 220,000 impactors greater than 50 m in diameter, while the Bland (2005) population contained about 3500 impactors greater than 50 m in diameter. During a single model run, this many impactors were randomly selected from the population; up to 10,000 runs were performed to derive a statistical average. The difference between these two populations is a measure of the current uncertainty in the terrestrial impactor size-frequency distribution and the disagreement between the observations of near-Earth objects (NEOs) and the terrestrial cratering record.

The depth-area distribution of oceans on the Earth was defined based on data from Stewart (2005). Ocean depth was divided into 1 km intervals, from 0 to 7 km; for each interval, the relative area of the Earth covered by water of that depth was calculated and used as the probability that an impact would occur in water at that depth interval. The values used are presented in Table 3. Exact water depths were selected at random with equal probability across the range of each interval.

To compute the final crater diameter from the impactor diameter and water depth, we used the following approach: we assumed a constant impact velocity (in this case equal to the mean asteroid impact velocity on Earth 18 km s^{-1}, to be consistent with previous crater size frequency estimates), impactor density (2700 kg m^{-3}), and impact angle (90°), and used scaling laws (Collins et al. 2005 and references therein) to compute first the transient crater diameter, then the final crater diameter. We then modified the final crater diameter using Equation 3 to account for the water depth (unless the final crater diameter was greater than 3.2 km—implying that the crater would be complex if formed in a target with no water layer—and the water depth exceeded 3.5 times the impactor diameter, in which case we did not adjust the final crater diameter and flagged the crater as an "impact-related resurge feature").

The transient crater diameter in the target with no water layer, D_{tc}, was calculated using:

$$D_{tc} = 1.161 L^{0.78} v^{0.44} g^{-0.22} \sin^{1/3}\theta \quad (6)$$

where L is the impactor diameter, v is the impactor velocity, g is the gravitational acceleration at the Earth's surface (9.81 ms^{-2}), and θ is the angle of impact to the horizontal (Collins et al. 2005 and references therein). Equation 6 assumes that the impactor and target density are the same. The equation relating transient and final crater diameter is dependent on whether the final crater is simple or complex (the transition is at D_{tc} = 2.56 km, corresponding to a final crater diameter of 3.2 km). For simple craters we used:

$$D_f = 1.25 D_{tc} \quad (7)$$

For complex craters we used:

$$D_f = 1.1 D_{tc}^{1.13} \quad (8)$$

The weakness of our model strategy is that it does not consider the effect of impact velocity and angle, which are likely to vary substantially from the constant values used (v = 18 km s^{-1}; θ = 90°). We could not include these variables explicitly because their effect on final crater diameter was not

constrained by our modeling work. Equation 3 was defined for an impact velocity of 15 km s^{-1} and should be valid at the slightly higher value of 18 km s^{-1}, but may not be valid for much higher or lower velocities. Equation 6 implies that a crater of a given size, formed in a dry target by an impactor with diameter L_1 and velocity v_1, could also be formed by a smaller, faster impactor, or a larger, slower impactor. If we now consider that these events occur in a water-covered target with a constant water depth, then in the higher-velocity case the impactor is smaller and so the ratio of the water depth to impactor diameter R is larger. Hence, according to Equation 2, the effect of the water layer will be stronger at higher impact velocity; in other words, the wet-target crater will be smaller relative to the dry-target crater in the higher-velocity case. More importantly, Equation 3 applies strictly only for vertical impacts. Impactors that strike at 45° to the target surface, which are much more common than near-normal incidence impacts, will penetrate about 1.5 times the volume of water traversed by an impactor striking at 90°. Thus, Equation 3 is likely to underestimate the reduction in final crater size caused by the presence of a water layer. It seems likely, therefore, that the inclusion of variable impact angle and impact velocity in our analysis would increase the filtering effect of the water layer relative to our simple model; the results that follow provide an upper limit on the size-frequency distribution of terrestrial craters.

Figure 7 shows the results of our statistical cratering model using the Bland (2005) impactor population (black lines) and the power-law impactor population (gray lines). Plotted on the graph are the predicted crater size-frequency distributions after 100 Ma for the whole Earth if it had no oceans (solid lines), for the whole Earth if it had its current ocean coverage (wide-dashed lines), for just the current terrestrial oceans (dotted), and for just the current continents (dashed). The effect of the oceans is to reduce in size the majority of craters forming on the Earth and completely prevent some craters from forming. This filtering and size reduction becomes less significant with increasing crater diameter, as the area of the Earth's oceans deep enough to affect these events is smaller. Also shown in Fig. 7 is the size-frequency distribution of terrestrial craters known to have formed in the last 100 million years (Grieve and Shoemaker 1995). The crater size-frequency distributions estimated using the Bland (2005) impactor population appear more consistent with observational data, suggesting that the power-law impactor population includes too many impactors in the 50–500 m range. The curves representing the size-frequency distribution of young craters on the oceans and continents suggest that we have probably already discovered all continental craters younger than 100 Ma and greater than 80–100 km in diameter, although a couple may remain undiscovered in the oceans. The modeled crater size-frequency distribution for the oceans suggests that approximately 100–200 craters larger than 10 km in diameter should be scarring the sea floor.

Table 3. Relative area of the Earth covered by water as a function of depth (adapted from Stewart 2005; values quoted to two significant figures).

Depth of water (km)	Percent of the total area of the Earth's surface
Land	29
0–1	8.3
1–2	3.2
2–3	6.0
3–4	16
4–5	22
5–6	15
6–7	0.61

Figure 8 shows the number of craters formed over 100 million years, divided into bins with a width of a factor of $2^{1/3}$ in diameter, as a function of diameter. Curves are plotted for the continents (wide-dashed lines) and the oceans (solid lines) as predicted by our model when using the Bland (2005) impactor population (black lines) and the power-law impactor population (gray lines). In the case of the Bland (2005) impactor population, the shape of the impactor size-frequency distribution (which is based on the observed lunar production population) leads to the number of craters on the ocean floor actually decreasing with decreasing crater size below about 6 km in diameter, implying that small oceanic craters may be particularly rare.

Figure 8 also shows the number of craters filtered out by the oceans (the number of craters prevented from forming by the ocean; dashed lines) and the number of resurge-dominated impact features (dotted lines) as a function of diameter for the two impactor populations. For both impactor populations, no craters larger than about 17 km in diameter are completely filtered out by the water layer due to the finite maximum depth of the oceans. Approximately 150–600 impact events may have formed an impact-related resurge feature instead of a crater; these events occur exclusively in the ~5–20 km diameter size range, and most often in water 2–4 km deep. The increase in the number of resurge features with increasing crater diameter (up to a maximum of ~12 km in diameter) is a consequence of the fact that the area of the Earth covered by oceans of a given depth increases dramatically with increasing water depth between 1 and 5 km (see Table 3). Hence, even though the probability of forming a given size crater on land decreases with increasing crater diameter, the probability of the impact creating a resurge feature 5–12 km in diameter instead of a crater increases with increasing crater diameter. The actual number of resurge features in the current oceans is likely to be strongly affected by the presence of weak sediments on the seabed. Future observational, experimental, and numerical modeling work is required to fully understand the nature of these impact events.

Figure 9 shows the predicted number of impact craters assuming the Earth has its current ocean coverage, divided by the predicted number of craters assuming a completely

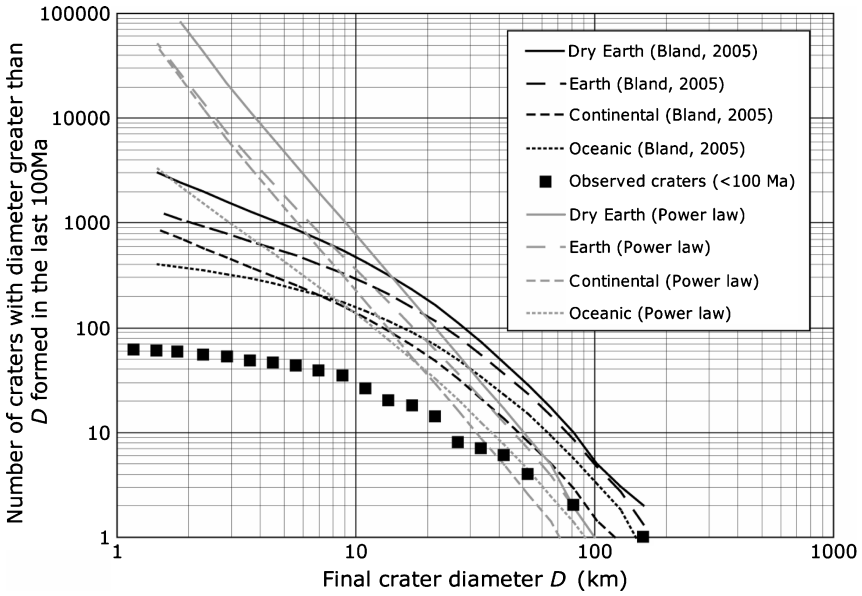

Fig. 7. The predicted cumulative size-frequency distribution of craters larger than 1 km in diameter that would form on Earth in a 100 Ma period. Black lines are for results calculated using the impactor population from Bland (2005); gray lines assume a power-law impactor size-frequency distribution derived from observational data. Solid lines represent a dry Earth case, assuming no oceans are present on the Earth. Wide-dashed lines are for the whole Earth with current ocean coverage. Dashed lines show the craters formed on the continents. Dotted lines show those craters that formed in the oceans. For comparison, the observed craters known to have formed in the past 100 Ma are also plotted (Grieve and Shoemaker 1995). Approximately 100–200 craters larger than 10 km in diameter should be found on the seafloor; only above this crater size does the probability of finding a crater younger than 100 Ma on the seafloor exceed that of finding a crater on land.

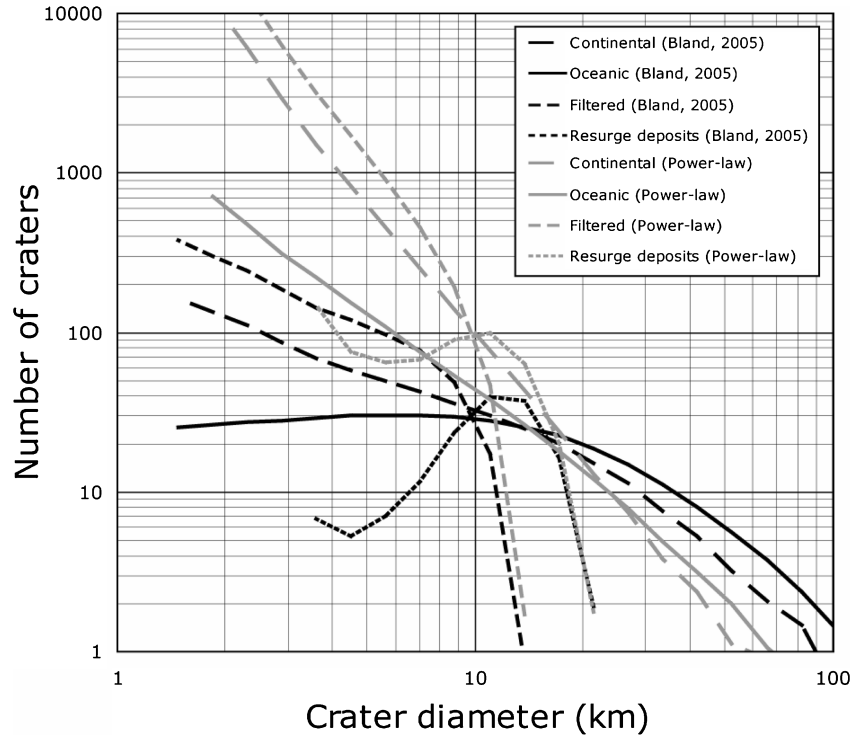

Fig. 8. The number of craters larger than 1 km in diameter predicted to have formed in a 100 Ma period as a function of crater diameter, binned according to crater size with a bin width of a factor of $2^{1/3}$ in crater diameter. Curves are shown for those craters that would form on continents (wide-dashed lines) and in the oceans (solid lines); also plotted are the number of resurge features created (dotted lines), which have diameters between ~3.5 km and ~20 km, and the number of craters filtered out by the water layer (dashed lines). No craters larger than ~17 km are filtered out. Black lines are for results calculated using the impactor population from Bland (2005) and gray lines assume a power-law impactor size-frequency distribution derived from observational data.

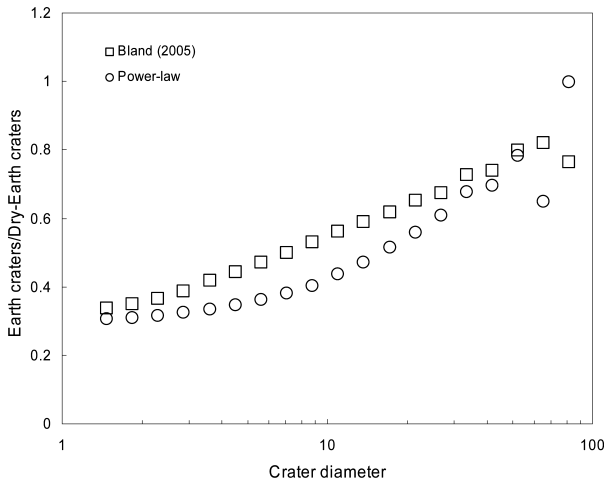

Fig. 9. Plot showing the predicted number of impact craters assuming the Earth has its current ocean coverage, divided by the predicted number of craters, assuming a completely dry Earth, as a function of crater diameter. Square symbols represent model results assuming an impactor population derived from Bland (2005); circles represent model results assuming a simple power-law impactor population. Two-thirds of craters smaller than 1 km in diameter are filtered out by the oceans, while one-third of craters about 30 km in diameter are filtered out.

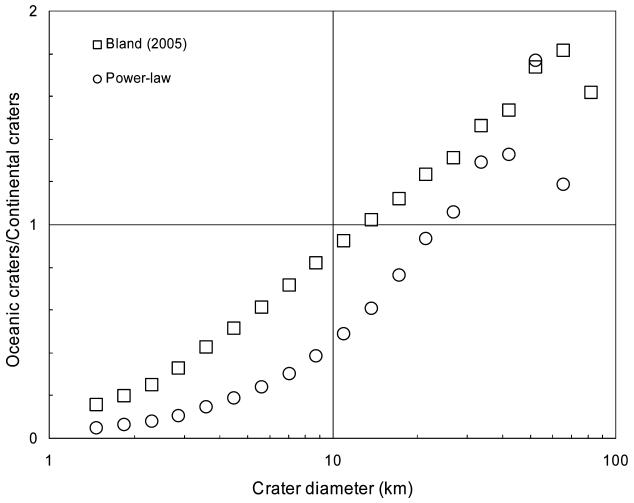

Fig. 10. Plot showing the predicted number of impact craters on the ocean floor divided by the number of continental craters as a function of crater diameter. Square symbols represent model results assuming an impactor population derived from Bland (2005); circles represent model results assuming a simple power-law impactor population. Craters smaller than ~12–25 km in diameter form more frequently on the continents than in the oceans. See text for further details.

dry Earth, as a function of crater diameter. The graph illustrates that the effect of the Earth's oceans is to reduce the number of craters smaller than 1 km in diameter by about two-thirds, the number of craters ~30 km in diameter by about one-third, and that for craters larger than ~100 km in diameter, the oceans have little effect. Figure 10 shows the ratio of continental impact craters to oceanic impact craters as a function of crater diameter as predicted by our model. For craters larger than approximately 12–25 km in diameter, more craters of that size occur on the ocean floor than on land due to the larger surface area of the oceans. However, the filtering effect of the water layer leads to more craters smaller than 12–25 km in diameter forming on land than on the ocean floor, despite only 30% of the Earth's surface being above sea level.

CONCLUSIONS

We have simulated over 60 marine impact events using a numerical model. Qualitatively, our model results agree well with previous work (Shuvalov 2002; Oberbeck et al. 1993). We identify three regimes of behavior (shallow water, intermediate water depth, and deep water), depending on the ratio of water depth to impactor diameter R and whether the impact forms a simple or complex crater.

1. The deep-water regime occurs for impacts where $R > 8$; in this case, all the impactor's energy goes toward forming a crater in the water layer, and no crater is formed on the ocean floor.
2. The intermediate-water-depth regime applies only for impacts forming complex craters in the range of $3–4 < R < 6–8$. In this highly complex regime, the seafloor is affected by the passage of the shock wave that forms when the impactor strikes the water, by high-velocity water resurge flows, and by the temporary removal of the substantial overburden of the water column. Based on our model results, it is unclear what the final manifestation of such seafloor disturbances might be, but it is likely to be broader than the equivalent crater had the impact occurred on land.
3. The shallow-water regime, which represents all other cases, is characterized by a decrease in crater diameter with increasing R but with little large-scale change in crater morphology.

Our model results provide the first quantitative relationships between impact crater size, impactor diameter, and water depth. We find that the dimensions of the transient cavity formed in the seafloor during marine-target impacts, relative to the dimensions of the cavity that would form in the absence of a water layer, can be estimated using existing scaling laws, corrected to account for the loss of kinetic energy during penetration of the water layer. This approximation is adequate up to water thicknesses six times larger than the impactor's diameter; in deeper water, this approximation greatly overestimates the dimensions of the cavity in the seafloor. For simulated craters that form in the shallow-water regime, we find that the final crater diameter decreases linearly with R; no crater is formed on the seafloor above $R = 8$. Our model results do not consider the effect of impact velocity, impact angle, or the presence of weak sediments on the seabed. In shallow

coastal regions with sediment-covered floors, a different relationship may hold. The quantitative relationships derived from our work should therefore be regarded as first-order estimates and not applied to impacts very different to those simulated.

Using the quantitative relationship between final crater diameter and the ratio of water depth to impactor diameter, we have calculated expected size-frequency distributions of craters on Earth that for the first time account for the presence of the oceans. The model used makes several necessary simplifications; however, given the uncertainty in estimates of the current terrestrial impactor population, we believe that several important conclusions can be drawn from our model results:

1. The presence of the oceans reduces the number of craters smaller than 1 km in diameter by about two-thirds, the number of craters about 30 km in diameter by about one-third, and for craters larger than ~100 km in diameter, the oceans have little effect.
2. More craters of a given size occur on the ocean floor than on land for craters larger than ~12 km in diameter; at diameters smaller than ~12 km, more craters form on land than on the ocean floor.
3. In the last 100 million years, about 150 impact events formed impact-related resurge features 5–20 km in diameter, or disturbances on the seafloor, instead of craters.

Acknowledgments–This work would not have been possible without the years of model development behind iSALE, for which we are indebted to Kai Wünnemann, Boris Ivanov, and Jay Melosh. We are grateful to Phil Bland and an anonymous reviewer for their constructive comments, which improved this paper. GSC was funded by NERC grant NE/B501871/1. This is IARC publication number 2007-0442.

Editorial Handling—Dr. Jens Ormö

REFERENCES

Amsden A. A., Ruppel H. M., and Hirt C. W. 1980. SALE: A simplified ALE computer program for fluid flow at speeds. Los Alamos National Laboratories Report LA-8095. Los Alamos, New Mexico: LANL. 101 p.

Artemieva N., Karp T., and Milkereit B. 2004. Investigating the Lake Bosumtwi impact structure—Insight from numerical modeling. *Geochemistry Geophysics Geosystems* 5:Q11016.

Artemieva N. A. and Shuvalov V. V. 2002. Shock metamorphism on the ocean floor (numerical simulations). *Deep-Sea Research II* 49:959–968.

Baldwin E. C., Milner D. J., Burchell M. J., and Crawford I. A. 2007. Laboratory impacts into dry and wet sandstone with and without an overlying water layer: Implications for scaling laws and projectile survivability. *Meteoritics & Planetary Science* 42. This issue.

Bland P. A. 2005. The impact rate on Earth. *Philosophical Transactions of the Royal Society A* 363:2793–2810.

Bland P. A. and Artemieva N. A. 2003. Efficient disruption of small asteroids by Earth's atmosphere. *Nature* 424:288–291.

Bland P. A. and Artemieva N. A. 2006. The rate of small impacts on Earth. *Meteoritics & Planetary Science* 41:607–631.

Bottke W. F. Jr., Nolan M. C., Greenberg R., and Kolvoord R. A. 1995. Collisional lifetimes and impact statistics of near-Earth asteroids. In *Hazards due to comets and asteroids*, edited by Gehrels T. Tucson, Arizona: The University of Arizona Press. pp. 337–357.

Collins G. S., Melosh H. J., and Ivanov B. A. 2004. Modeling damage and deformation in impact simulations. *Meteoritics & Planetary Science* 39:217–231.

Collins G. S., Melosh H. J., and Marcus R. A. 2005. Earth Impact Effects Program: A Web-based computer program for calculating the regional environmental consequences of a meteoroid impact on Earth. *Meteoritics & Planetary Science* 40:817–840.

Collins G. S., Melosh H. J., Morgan J. V., and Warner M. R. 2002. Hydrocode simulations of Chicxulub crater collapse and peak ring formation. *Icarus* 157:24–33.

Collins G. S. and Wünnemann K. 2005. How big was the Chesapeake Bay impact? Insight from numerical modeling. *Geology* 33:925–928.

Dalwigk I. von and Ormö J. 2001. Formation of resurge gullies at impacts at sea: The Lockne crater, Sweden. *Meteoritics & Planetary Science* 36:359–369.

Dence M. R. 1965. The extraterrestrial origin of Canadian craters. *Annals New York Academy of Sciences* 123:941–969.

Gault D. E. and Sonett C. P. 1982. Laboratory simulation of pelagic asteroid impact: Atmospheric injection, benthic topography, and the surface wave radiation field. In *Geological implications of impacts of large asteroid and comets on the Earth*, edited by Silver L. T. and Schultz P. H. GSA Special Paper #190. Boulder, Colorado: Geological Society of America. pp. 69–92.

Grieve R. A. F. and Shoemaker E. M. 1995. The record of past impacts on Earth. In *Hazards due to comets and asteroids*, edited by Gehrels T. Tucson, Arizona: The University of Arizona Press. pp. 417–462.

Halliday I., Griffin A. A., and Blackwell A. T. 1996. Detailed data from 259 fireballs from the Canadian camera network and inferences concerning the influx of large meteoroids. *Meteoritics & Planetary Science* 31:185–217.

Ivanov B. A. 2005. Numerical modeling for the largest terrestrial impact craters. *Solar System Research* 39:426–456.

Ivanov B. A., Deniem D., and Neukum G. 1997. Implementation of dynamic strength models into 2-D hydrocodes, applications for atmospheric break-up and impact cratering. *International Journal of Impact Engineering* 17:375–386.

Ivanov B. A. and Artemieva N. A. 2002. Numerical modeling of the formation of large impact craters. In *Catastrophic events and mass extinctions: Impact and beyond*, edited by Koeberl C. and MacLeod K. GSA Special Paper #356. Boulder, Colorado: Geological Society of America. pp. 619–629.

Ivanov B. A. and Deutsch A. 1999. Sudbury impact event: Cratering mechanics and thermal history. In *Large meteorite impacts and planetary evolution II*, edited by Dressler B. O. and Sharpton V. I. GSA Special Paper #339. Geological Society of America pp. 389–397.

Kyte F. T., Zhou Z., and Wasson J. T. 1981. High noble metal concentrations in a late Pliocene sediment. *Nature* 292:417–420.

Melosh H. J. 1989. *Impact cratering: A geologic process*. New York: Oxford University Press. 245 p.

Melosh H. J. and Ivanov B. A. 1999. Impact crater collapse. *Annual Review of Earth and Planetary Sciences* 27:385–415.

Near-Earth Object Science Definition Team. 2003. Study to

determine the feasibility of extending the search for near-Earth objects to smaller limiting diameters. NASA Technical Report. 166 p.

Nemtchinov I. V., Loseva T. V., and Teterev A. V. 1996. Impacts into oceans and seas. *Earth, Moon, and Planets* 72:405–418.

Oberbeck V. R., Marshall J. R., and Aggarwal H. 1993. Impacts, tillites, and the breakup of Gondwanaland. *The Journal of Geology* 101:1–19.

O'Keefe J. D. and Ahrens T. J. 1982. The interaction of the Cretaceous/Tertiary extinction bolide with the atmosphere, ocean, and solid Earth. In *Geological implications of impacts of large asteroid and comets on the Earth*, edited by Silver L. T. and Schultz P. H. GSA Special Paper #190. Boulder, Colorado: Geological Society of America. pp. 103–109.

Ormö J. and Lindström M. 2000. When a cosmic impact strikes the sea bed. *Geological Magazine* 137:67–80.

Ormö J. and Miyamoto H. 2002. Computer modelling of the water resurge at a marine impact: The Lockne crater, Sweden. *Deep-Sea Research II* 49:983–994.

Ormö J., Shuvalov V. V., and Lindström M. 2002. Numerical modeling for target water depth estimation of marine-target impact craters. *Journal of Geophysical Research* 107:3.1–3.9.

Poag C. W. 1996. Structural outer rim of Chesapeake Bay impact crater: Seismic and borehole evidence. *Meteoritics & Planetary Science* 31:218–226.

Poag C. W., Koeberl C., and Reimold, W. U. 2004. *The Chesapeake Bay crater—Geology and geophysics of a Late Eocene submarine impact structure*. Heidelberg: Springer. 522 p.

Schmidt R. M. and Housen K. R. 1987. Some recent advances in the scaling of impact and explosion cratering. *International Journal of Impact Engineering* 5:543–560.

Shuvalov V. V. 1999. Multi-dimensional hydrodynamic code SOVA for interfacial flows: Application to the thermal layer effect. *Shock Waves* 9:381–390.

Shuvalov V. V. 2002. Numerical modeling of impacts into shallow sea. In *Impacts in Precambrian shields*, edited by Plado J. and Pesonen L. J. New York: Springer-Verlag. pp. 323–336.

Shuvalov V., Dypvik H., and Tsikalas F. 2002. Numerical simulations of the Mjølnir marine impact crater. *Journal of Geophysical Research* 107:1-1–1-3.

Shuvalov V. V. and Trubestkaya I. A. 2002. Numerical modeling of marine target impacts. *Solar System Research* 36:417–430.

Stewart R. H. 2005. Introduction to physical oceanography. http://oceanworld.tamu.edu/resources/ocng_textbook/contents.html. Accessed October 15, 2006.

Tsikalas F. 1996. A geophysical study of Mjølnir: A proposed impact structure in the Barents Sea. Ph.D. thesis, University of Oslo, Oslo, Sweden.

Wünnemann K., Collins G. S., and Melosh H. J. 2006 A strain-based porosity model for use in hydrocode simulations of impacts and implications for transient crater growth in porous targets. *Icarus* 180:514–527.

Wünnemann K. and Ivanov B. A. 2003. Numerical modelling of the impact crater depth-diameter dependence in an acoustically fluidised target. *Planetary and Space Science* 51:831–845.

Wünnemann K. and Lange M. A. 2002. Numerical modeling of impact induced modifications of the deep-sea floor. *Deep-Sea Research II* 49:969–981.

Wünnemann K., Morgan J. V., and Jödicke H. 2005. Is Ries crater typical for its size? An analysis based upon old and new geophysical data and numerical modeling. In *Large meteorite impacts III*, edited by Kenkmann T., Hörz F., and Deutsch A. GSA Special Paper #384. Boulder, Colorado: Geological Society of America. pp. 67–83.